JOURNAL OF MATERIALS SCIENCE **20** (1985) 3421–3427

Thermal shock resistance of Mg–PSZ

A. H. HEUER, L. H. SCHOENLEIN*
Department of Metallurgy and Materials Science, Case Institute of Technology, Case Western Reserve University, Cleveland, Ohio 44106, USA

The thermal shock resistance (TSR) of Mg–PSZ (a partially stabilized ZrO_2) containing either tetragonal t- or monoclinic m-ZrO_2 precipitates was studied. The samples containing t-ZrO_2 had superior TSR, particularly in having a higher retained strength after thermal fracture had been initiated. The t-ZrO_2 in the surface regions of shocked samples transformed to a new polymorph with orthorhombic (o) symmetry; the stress-induced t → o transformation may be responsible in part for the improved TSR in samples containing t-ZrO_2 compared to those in which all the particles have m symmetry.

1. Introduction

The thermal shock resistance (TSR) of partially stabilized ZrO_2 (PSZ) is an important property for many current or anticipated applications. Since the recognition of transformation toughening in these materials [1–4], however, there have been few studies of the change in TSR with microstructural development. Swain and co-workers [5, 6] have shown that good TSR against quenching in water can be had in Mg–PSZ by heat-treating samples to develop either "peak-aged" microstructures (these are comparable to Porter and Heuer's "optimally-aged" microstructures [2, 3]) or "sub-eutectoid" microstructures; only the latter microstructure was effective in providing TSR against up-quenching into molten aluminium at 900° C. This was attributed to *R*-curve behaviour and the improved high-temperature K_{IC} derived from the sub-eutectoid heat treatment. However, Swain and co-workers [5, 6] have not given any detailed explanation of the optimization of TSR with peak ageing in this particular form of PSZ, aside from the general optimization due to transformation toughening. Such a microstructure-based explanation was attempted earlier by Schoenlein [7], who suggested that thermal stresses at specimen surfaces were relieved in water-quenched Mg–PSZ by the tetragonal to monoclinic (t → m) transformation, and (similar to Swain *et al.* [5]) by interaction of thermally-initiated cracks with untransformed t-ZrO_2 particles. We have now discovered [8–10] that surface transformation of t-ZrO_2 does indeed occur, but that the transformation product is not the usual stress-induced m-ZrO_2, but a new ZrO_2 polymorph with orthorhombic (o) symmetry. (Note that this is not the high-pressure polymorph of ZrO_2 which also is orthorhombic [11].) The present paper summarizes Schoenlein's data and attempts to discuss the TSR of Mg–PSZ in terms of both the t → o and t → m transformations.

2. Experimental procedures and microstructural characterization

As in earlier work from our laboratory, the starting material for our study was a commercial Mg–PSZ containing 8.1 mol % MgO (No. 1027, Zircoa Division of Corning Glass Works, Solon, Ohio). Characterization of this material by transmission electron microscopy (TEM) can be found in [3]. The material was solution heat-treated at 1850° C in argon for 4 h, cooled rapidly to room temperature, and reheated (aged) in air at 1400° C for either 3 or 6 h. The average grain size increased from 53 μm in the as-received material to 63 μm in the solution-annealed state, and to 70 μm and 72 μm respectively after the 3 and 6 h ageings at 1400° C.

The solution-annealed materials had a thin surface layer which was depleted in MgO and

---

*Present address: EG & G, Idaho Falls, Idaho, USA.

0022–2461/85 $03.00 + .12

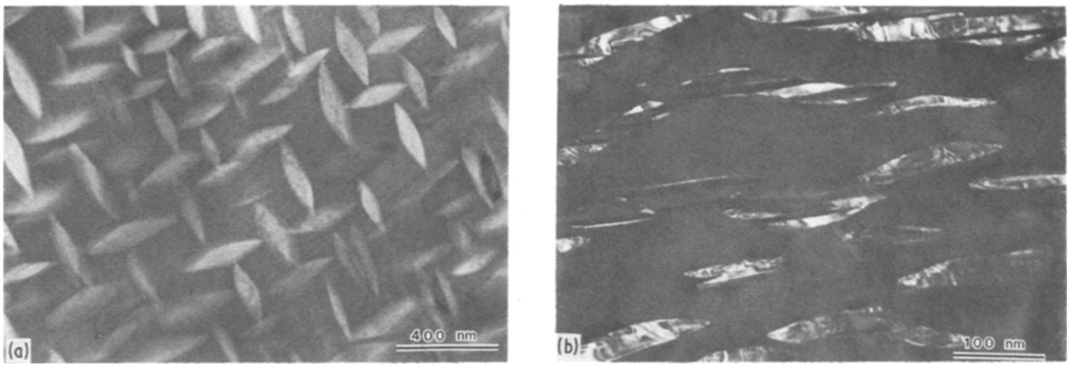

Figure 1 Bright-field micrographs of particles in heat-treated Mg–PSZ. (a) An example of the 3 h sample; all particles have t symmetry. (b) The corresponding 6 h sample; all particles have m symmetry.

contained appreciable amounts of m-ZrO_2. This formed because of surface evaporation of MgO during solution annealing, as the average composition of the surface moved from the single-phase cubic (c) field to the two-phase (c + t) field; the t particles grew beyond the critical size and transformed to m symmetry during cooling from 1850° C. Further work was done on samples from which the MgO-depleted layer was removed by polishing with 6 μm diamond paste.

During cooling following solution annealing, the bulk of the c grains precipitated small t-ZrO_2 particles which could be imaged by TEM (see Fig. 6 of [4]). X-ray analysis, using Porter and Heuer's modification [3] of Garvie and Nicholson's technique [12] on bulk samples pulverized to induce the t → m transformation, revealed that the solution heat-treated materials contained at least 3 vol % t-ZrO_2. (This is a lower bound, as it is possible that the finest particles remained untransformed and thus would not have been detected by the X-ray analysis.)

The microstructures of the sampled aged for 3 and 6 h are shown in Fig. 1; the particles all have t symmetry after 3 h and m symmetry after 6 h. X-ray analysis revealed 14 vol % t-ZrO_2 after 3 h and 18 vol % after 6 h; this should be compared with the amount predicted by the lever rule for an 8 mol % Mg–PSZ from the equilibrium phase diagram [13], which is 42% t-ZrO_2 at 1400° C. Sufficient coarsening has occurred during the pro-eutectoid precipitation of t-ZrO_2 in this system at 1400° C that when about 40% of the reaction is complete, the martensite start temperature (*Ms*) has increased to above room temperature. (It has been speculated [14, 15] that the increase in *Ms* occurs when particles lose coherency during ageing.)

During the latter portion of the study, we discovered that MgO evaporation also occurred during the 1400° C ageing and again resulted in a surface layer containing m-ZrO_2. The outermost portion of the specimen was probably 100% m-ZrO_2 – the evaporation during ageing caused the composition to decrease to that corresponding to the t-solvus – but even deep in the MgO-depleted layer, the driving force for precipitation of t-ZrO_2 must have been sufficiently high that significant coarsening occurred, resulting in particles with a high *Ms**. One series of samples was aged for 3 h at 1400° C while buried in MgO powder, which suppressed MgO evaporation sufficiently that no m-ZrO_2 formed in surface regions. X-ray analysis showed that this sample also contained 14 vol % t-ZrO_2.

The depth of the layer containing m-ZrO_2 was determined in the following way. A portion of the surface was ion-thinned for various times, with intermitant X-ray diffraction patterns being taken. The presence and amount of m-ZrO_2 could readily be determined from $\{1\,1\,1\}_{c\rightarrow t}$ and $(1\,1\,1)_m$ reflections, which were correlated with the depth of milling as measured by the amount

---

*A somewhat similar occurrence was found in grain boundary regions in samples aged for sufficiently short times that the bulk grains contained only t-ZrO_2. Sufficient silicon impurity was present in our starting material that forsterite (Mg_2SiO_4) formed as a grain-boundary phase. The regions adjacent to the grain-boundary was therefore depleted in MgO but remained within the two-phase (c + t) field. The increased driving force for the information of t-ZrO_2 led to larger particles near the grain-boundary, which had an *Ms* above room temperature.

TABLE I Mechanical properties of Mg–PSZ

Specimen	Average grain size (μm)	σ (MPa)*	K_{IC} (MPa m$^{-1/2}$)	c-ZrO$_2$ (vol %)
As-received	53	460	3.9	62
Solution-annealed	63	260	3.2	97
Air-aged (3 h)	70	400	4.9	86
Air-overaged (6 h)	72	350	4.5	82
MgO-aged (3 h)	–	450	–	86

*The samples were 25 mm × 5 mm × 2.5 mm and were tested in four-point bending.

of defocus on a calibrated optical microscope. The MgO-depleted zone vanished at a depth of 25 μm.

The Evans–Charles technique [16] was used to measure fracture toughness. No difficulty was found in measuring the toughness K_c, even in samples with a surface layer containing m-ZrO$_2$, and the length of well-developed cracks emanating from Vickers indent corners could be measured. The toughness was then found from the equation.

$$K_c = \frac{0.15Ha^{1/2}k}{\phi}\left(\frac{c}{a}\right)^{-3/2} \qquad (1)$$

where c and a are, respectively, half the indent diagonal plus the total crack length and half the indent diagonal; H is the microhardness, k a constraint factor ($=3.2$) and ϕ a second constraint factor ($=3.0$). Ten "good" indents were used for each K_c determination, a good indent being defined as one where cracks emanated from each corner of the indent. The toughness of the samples aged while buried in MgO could not be determined because small quantities of MgO powder sintered to the bars during ageing and obscured the measurement of crack length.

3. Results and discussion

3.1. Mechanical properties

The room-temperature mechanical properties of the specimens used for this study are shown in Table I. The 95% confidence interval for these and other data in this paper is ±25 MPa (Fig. 2). The results are in general accord with the prior literature, particularly the effect of heat treatment on strength σ_f. The heat treatments chosen for studying TSR (3 and 6 h) were respectively less than and greater than that yielding a maximum strength (4 h at 1400° C, for which we found σ_f to be 500 MPa). This was done so as to obtain samples with roughly comparable strengths but different microstrutures. Swain *et al.* [5] found σ_f to be 600 MPa for ground, peak-aged samples but 500 MPa for polished peak-aged samples. This agrees with our data in that our specimens, which were polished before ageing and given no further surface treatment, should be compared with the polished samples of Swain *et al.* [5].

The TSR of Mg–PSZ is shown in Fig. 2, which shows the retained strength at room temperature after water quenching plotted against quench temperature. The critical temperature

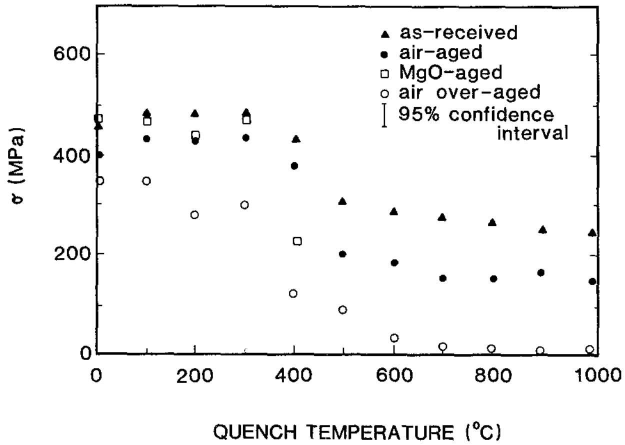

Figure 2 Thermal shock resistance of Mg–PSZ.

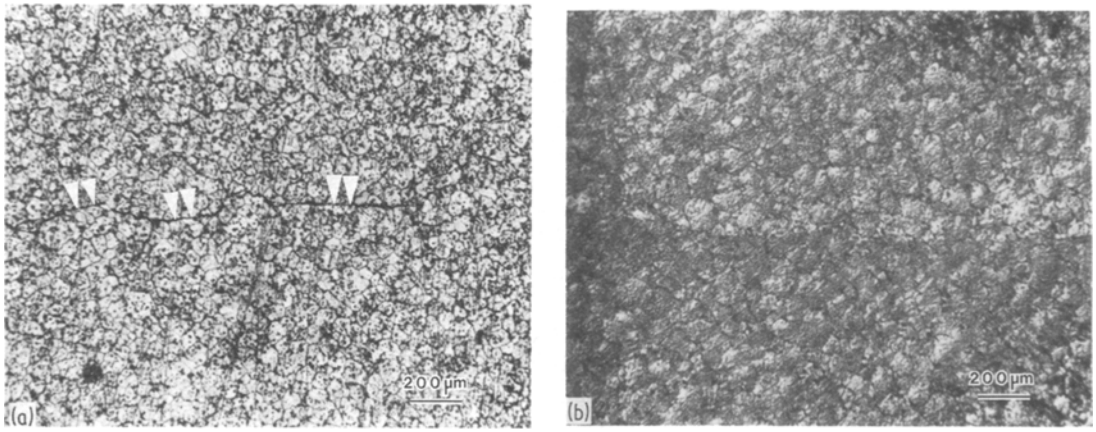

Figure 3 Microstructure of thermally-shocked samples; (a) a thermally-induced crack (arrowed) on the thermally-etched surface, seen to have propagated both inter- and trans-granularly; (b) the same area under Nomarski interference contrast, revealing the surface roughening that accompanied thermal shock in air-aged specimens.

difference that induces marked weakening, ΔT_c, for the samples containing t-ZrO_2 (the as-received and 3 h-aged samples) appear to be higher than for the over-aged samples containing only m-ZrO_2. The sparsity of our test data prevented us from determining ΔT_c accurately, but our data are in agreement with values of Swain *et al.* of 340, 420, and 300° C for ground as-fired, ground peak-aged, and ground over-aged specimens respectively, and 350° C for polished peak-aged samples. The presence of t-ZrO_2 appears to increase ΔT_c by 50 to 100° C. It should also be noted that only samples containing t-ZrO_2 have a reasonable retained strength after shocking from $\Delta T > \Delta T_c$. Finally, we note that the as-received specimens had the highest after-shock strength; this may be related to their finer grain size.

One set of as-received, one set of air-aged, and one set of MgO-aged samples were quenched five times using a ΔT of 300° C ($< \Delta T_c$), prior to measuring the retained room-temperature strength. All three sets of samples had an average strength of 180 MPa, roughly equal to the strength of samples shocked from $\Delta T > \Delta T_c$. It is clear that severe thermal-initiated fracture had occurred in all specimens, and that Mg–PSZ does not possess multi-shock TSR.

3.2. Microstructural characterization of thermally shocked specimens

The microstructures of thermally-shocked specimens have been characterized using optical microscopy of the originally-polished surfaces, fractography and conventional TEM. These characterizations will be described in turn.

Fig. 3a shows the microstructure of an air-aged specimen quenched from 400° C. Thermal stress-induced cracks are present, and can be seen to have propagated both inter-granularly and trans-granularly. (The microstructure was readily observed because the polished, solution-annealed material underwent thermal etching during the 1400° C ageing.) Such thermal-shock induced fracture initiation coincided with the onset of strength degradation, the crack density increasing with increasing ΔT.

Fig. 3b shows the same area as Fig. 3a, but under Nomarski interference contrast. The surface roughening thus revealed was also coincident with initiation of thermal fracture, but only in air-aged specimens; as-received and MgO-aged specimens showed only cracking. This roughening is similar to that found by El-Shiekh and Nicholson [17] in Ca–PSZ, and is thought to be associated with spalling of the MgO-depleted layer rich in m-ZrO_2 that is present on air-aged specimens.

Fractographic analysis of an unshocked air-aged and an unshocked air-overaged specimen tested at room temperature revealed that both types of specimen had undergone primarily trans-granular fracture, although the surface of the sample containing t-ZrO_2 was somewhat rougher in appearance. The roughness is expected due to the significant interaction between propagating cracks and transforming particles,

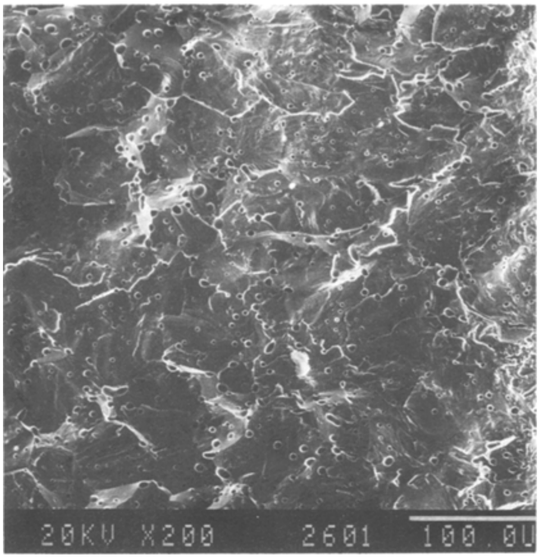

Figure 4 Fractograph of MgO-aged sample shocked from 400° C (note that the sample was tested at room temperature). The trans-granular fracture surface was also characteristic of unshocked samples. Scale bar = 100 μm.

and has been observed previously in Mg–PSZ [18, 19].

A fractograph of a MgO-aged sample shocked from 400° C is shown in Fig. 4; the fracture mode is to all intents and purposes trans-granular, and identical to that of the unshocked air-aged specimens. On the other hand, Fig. 5 shows fractographs of specimens air-aged (Fig. 5a) or air-overaged (Fig. 5b) after shocking from 1000° C. The fracture mode is now distinctly inter-granular. This could have resulted from (a) a "weakening" of the grain boundaries by the sizeable thermal stresses, or (b) be a manifestation of crack propagation at a lower fracture stress [20], or (c) reflect the fact that much of the fracture surface of Fig. 5 was formed from thermally-induced cracks while the specimen was still at elevated temperatures. Swain [21] has shown that the fracture morphology of Mg–PSZ changes from trans-granular to inter-granular at about 450° C.

Finally, as mentioned in Section 1, thermal stresses induced a transformation from t to o symmetry in the air-aged and MgO-aged materials*. The new o-ZrO_2 polymorph is shown in Fig. 6 in a back-thinned foil; it only occurs within 10 to 20 μm of the surface, and the volume increase associated with the t $\rightarrow$ o transformation is about 1% [10]. This new phase was present in surface regions of samples quenched from 200, 400 and 1000° C and may even occur at thermal stresses as small as that associated with a 100° C quench. (We have not attempted to calculate the magnitude of these stresses as a function of ΔT in Mg–PSZ because of the unknown heat transfer coefficients attendant on quenching Mg–PSZ into water.)

It is possible that the higher ΔT_c in samples containing t-ZrO_2 precipitates is due in part to the t $\rightarrow$ o transformation relieving thermal stresses. This notion (speculative at present) is consistent with the poor "multi-shock" TSR described in the previous section, in that the high surface tensile stresses in the second and subsequent cycles cannot be relieved except by crack propagation; no t-ZrO_2 is available in the surface

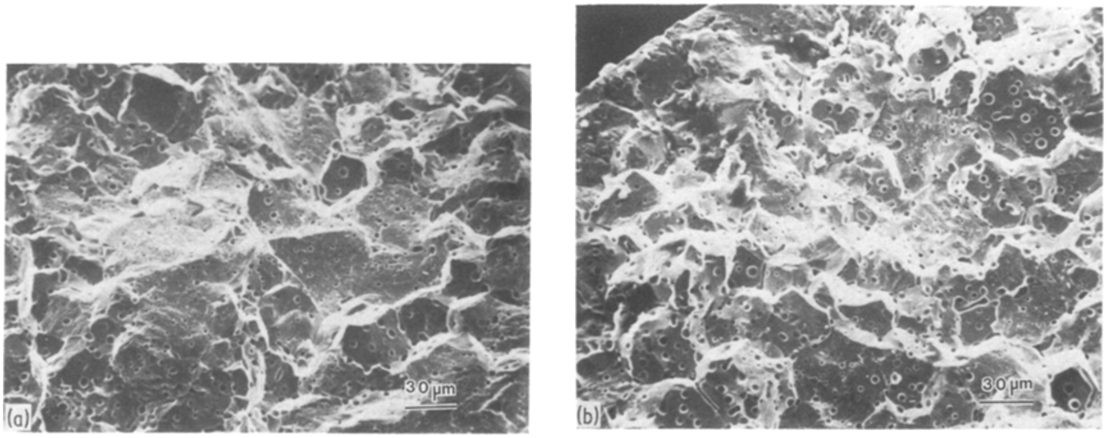

Figure 5 Fractographs of specimens shocked from 1000° C: (a) the fracture surface of a sample air-aged for 3 h; (b) a sample air-aged for 6 h.

---

*It probably is also present in thermally-shocked as-received specimens, but these have not been studied.

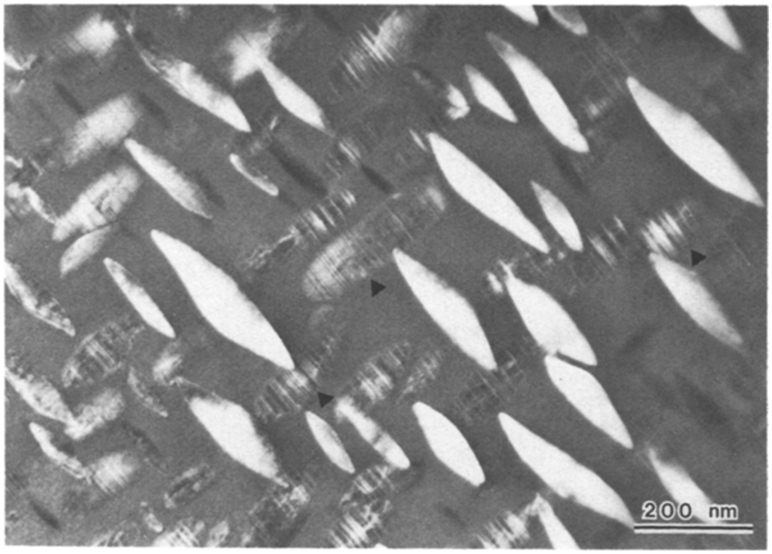

Figure 6 o-ZrO_2 particles in the near-surface regions of an MgO-aged specimen quenched from 400° C. The internal structure (arrowed) has been shown to be due to two o-ZrO_2 structures, one with c ~ 0.5 nm, the other with c ~ 1 nm [9, 10].

regions experiencing high biaxial tension that could undergo the t → o transformation, and the thermal stresses are not high enough to induce the o → m transformation which has been shown to occur in crack-tip stress fields [8, 22]. No m-ZrO_2 could be detected by X-ray diffraction in the surface regions of multiply-shocked MgO-aged specimens.

Lewis and Rice [23] have previously tested the same commercial Mg–PSZ under multi-shock conditions. They found that the onset of damage was little affected by multiple shocks, especially compared to materials thought to undergo microcracking. This contrary finding may be explained by the fact that their specimens differed from ours in having been ground with a 180-grit metal-bonded diamond wheel. On the other hand, since the microstructure and resulting mechanical behaviour is quite sensitive to cooling history following sintering, the materials they tested may be unlike any used in the present investigation. These workers have shown, however, that the thermal fatigue seen here is not likely to be a result of conventional stress-corrosion cracking.

The interior of all thermally shocked specimens, which of course were loaded compressively during water quenching, had the same microstructure as unshocked specimens. The presence of untransformed t-ZrO_2 particles in the as-received, air-aged, and MgO-aged transformation-toughened ceramics is the reason for the high post-shock strength noted above. In this regard, the overaged specimen is quite different. While its strength and toughness before thermal shock were reasonable, and must reflect crack deflection or microcrack toughening, it has little resistance to crack extension once thermally-initiated fracture has ensued.

4. Conclusions

The thermal shock resistance of Mg–PSZ containing t-ZrO_2 precipitates is significantly improved over similar materials where the particles are larger and have m symmetry. The ΔT_c above which significant strength degradation occurs upon quenching into water is increased, and the retained strength for $\Delta T > \Delta T_c$ is significantly higher by a factor of five to ten. The increase in ΔT_c may be caused in part by a stress-induced t → o transformation which occurs at specimen surfaces and relieves thermal tensile stresses. The improved strengths for $\Delta T > \Delta T_c$ is attributed to untransformed t-ZrO_2 in the bulk of the specimens, which imparts the usual transformation toughening.

Acknowledgements

This research was supported by the National Science Foundation under Grant No. DMR 77–19163. A. H. Heuer thanks the Alexander von Humboldt Foundation for a Senior Scientist Award, which made possible his sabbatical leave at the Max Planck Institut für Metallforschung, Stuttgart, FRG, where this paper was written.

References

1. R. C. GARVIE, R. H. J. HANNICK and R. T. PASCOE, *Nature* **258** (1975) 703.
2. D. L. PORTER and A. H. HEUER, *J. Amer. Ceram. Soc.* **60** (1977) 183.
3. *Idem, ibid.* **62** (1979) 183.
4. A. H. HEUER, "Advances in Ceramics 3: Science and Technology of Zirconia", edited by A. H. Heuer and L. W. Hobbs (The American Ceramic Society, Columbus, Ohio, 1981) p. 98.
5. M. V. SWAIN, R. C. GARVIE, R. H. J. HANNICK, R. HUGHAN and M. MARMACK, *Proc. Brit. Ceram. Soc.* **31** (1983) 343.
6. M. V. SWAIN, "Fracture Mechanics of Ceramics 6", edited by R. C. Brandt, A. G. Evans, D. P. H. Hasselman and F. F. Lange (Plenum Press, New York, 1983) p. 355.
7. L. H. SCHOENLEIN, MS thesis, Case Western Reserve (1979).
8. L. H. SCHOENLEIN and A. H. HEUER, "Fracture Mechanics of Ceramics 6", edited by R. C. Brandt, A. G. Evans, D. P. H. Hasselman and F. F. Lange (Plenum Press, New York, 1983) p. 309.
9. A. H. HEUER, L. H. SCHOENLEIN and S. FARMER, "Science of Ceramics", Vol. 12, edited by P. Vincenzini (Ceramurgia, s.r.l., Faenza, Italy, 1984) p. 257.

H. SCHOENLEIN and A. H. HEUER, to be ublished.

-G. LIU, *J. Phys. Chem. Solids* **41** (1980) 331.

12. C. GARVIE and P. S. NICHOLSON, *J. Amer. Ceram. Soc.* **55** (1972) 303.
13. C. F. GRAIN, *ibid.* **50** (1967) 228.
14. R. H. J. HANNINK, *J. Mater. Sci.* **13** (1978) 2487.
15. A. H. HEUER, N. CLAUSSEN, W. M. KRIVEN and M. RÜHLE, *J. Amer. Ceram. Soc.* **65** (1982) 642.
16. A. G. EVANS and E. A. CHARLES, *ibid.* **59** (1976) 371.
17. A. M. EL-SHIEKH and P. S. NICHOLSON, *ibid.* **57** (1979) 19.
18. D. L. PORTER, G. K. BANSAL and A. H. HEUER, *ibid.* **59** (1976) 179.
19. D. L. PORTER and A. H. HEUER, *ibid.* **60** (1977) 280.
20. A. H. HEUER, *ibid.* **52** (1969) 510.
21. M. V. SWAIN, unpublished research.
22. L. K. LENZ and A. H. HEUER, *J. Amer. Ceram. Soc.* **65** (1982) C192.
23. D. LEWIS and R. W. RICE, *Ceram. Engng. Sci. Proc.* **2** (1981) 712.

Received 6 August
and accepted 10 September 1984